

Polymer Thin Films on Patterned Si Surfaces

Z. Li,^{†,‡} M. Tolan,[§] T. Höhr,[†] D. Kharas,[†] S. Qu,[†] J. Sokolov,^{*,†} M. H. Rafailovich,^{*,†} H. Lorenz,^{||} J. P. Kotthaus,^{||} J. Wang,[⊥] S. K. Sinha,[⊥] and A. Gibaud[&]

Department of Materials Science and Engineering, State University of New York at Stony Brook, Stony Brook, New York 11794-2275, Institut für Experimentalphysik der Universität Kiel, Leibnizstrasse 19, 24098 Kiel, Germany, Sektion Physik, Ludwig-Maximilians-Universität München, Geschwister-Scholl-Platz 1, 80539 München, Germany, Argonne National Laboratory, APS, 9700 South Cass Avenue, Argonne, Illinois 60439-4814, and Faculte des Sciences, Universite du Maine, 72017 LeMans Cedex, France

Received July 2, 1997; Revised Manuscript Received January 5, 1998

ABSTRACT: The propagation of roughness from a patterned silicon surface by polymer thin films was measured as a function of film thickness, time, and surface interaction using atomic force microscopy and synchrotron X-ray reflection. In the presence of an interacting surface, the decay length of the surface modulation was much longer than that observed in simple liquids. By measuring the time dependence of the surface corrugation amplitude, we were able to extract a surface diffusion coefficient by applying a modified version of the Mullins theory for surface diffusion in crystalline solids. The measured diffusion coefficients were an order of magnitude smaller than in the bulk, and scaled as $1/M^{3/2}$, in agreement with previous SIMS results. The results are interpreted in terms of surface interactions confining polymer chains over distances larger than the radii of gyration.

Introduction

Thin polymer films are of great importance in a large body of technological applications, e.g., coatings on optical surfaces, supermirrors, and waveguides.¹ One common problem in preparing uniform high quality films is the propagation of the substrate roughness to the topmost film surface. The surface roughness of a simple liquid film was studied by Tidswell et al.² They showed that the correlation of surface roughnesses with the substrate roughness was strongly damped, becoming undetectable for films thicker than about 100 Å. This result was shown to agree with the theory of Andelmann, Joanny, and Robbins³ (AJR) where the structure factor for the surface roughness in a simple liquid is calculated by balancing the van der Waals interaction between the molecules and the corrugated surface with smoothing tendency driven by surface tension.

Due to the complex nature of the individual molecules, the behavior of polymeric liquids can be very different from that of simple liquids. In the vicinity of an ideal noninteracting surface, the chains are free to move along the surface and Aussere,⁴ Grannick,⁵ and others⁶ have shown that no additional force is required to compress the chains. For an interacting surface, on the other hand, the chains can be pinned and the entropic penalty associated with specific configurations must be considered when discussing interfacial phenomena. Additional terms describing the entropic contribution to the free energy have been shown previously to account for anomalies in the wetting behavior of entangled polymer films, such as surfaces possessing a film thickness dependence of the spreading parameters⁷ and autopho-

bicity between layers of chemically identical materials.⁸ Recently several groups have reported anomalous glass transition behavior^{9,10} or reduced chain mobility¹¹ near interacting surfaces.

In this paper we show that confinement effects can also dominate the polymer liquid structure factor and the surface spreading dynamics, which together strongly impact on the propagation of substrate roughness in thin homopolymer film coatings. Finally, we also show how the dynamics of surface smoothing can be a simple way to measure lateral surface diffusion on a polymer thin film.

The model system we used was that of monodisperse polystyrene (PS) and poly(methyl methacrylate) (PMMA) thin films on laterally structured silicon (Si) substrates (i.e., surface gratings). These gratings can be regarded as surfaces possessing a particular type of roughness with only a few enhanced Fourier components in the wavenumber spectrum. The adsorbed polymer film can then follow the periodic structure in a well-specified manner. Hence, in contrast to previous experiments on the thin liquid films, which were performed on randomly rough surfaces, the conformal part is now clearly separated from the statistical microscopic roughness. If the equilibrium and kinetic properties are both probed, a direct comparison with existing theories is now greatly simplified since the small scale internal substructure of the polymer films can introduce random roughness unrelated to the substrate.

If $\Gamma_S(q)$ denotes the Fourier transform of the substrate contour and $\Gamma_L(q)$ is the Fourier transform of the surface, then a linear response theory yields the result $\Gamma_L(q) = \chi(q, l) \Gamma_S(q)$. The response function $\chi(q, l)$, which depends on the wave vector q and the film thickness l connects both surfaces and describes how the substrate roughness is replicated by the adsorbed film. The AJR microscopic theory for $\chi(q, l)$ of simple liquids, in the Deryagin approximation,⁹ yields the prediction^{3,10}

* To whom correspondence should be addressed.

[†] State University of New York at Stony Brook.

[‡] Present address: Exxon Research and Engineering Company, Route 22 East, Annandale, NJ08865.

[§] Universität Kiel.

^{||} Ludwig-Maximilians-Universität München.

[⊥] Argonne National Laboratory.

[&] Universite du Maine.

$$\chi(q, l) = \frac{a^2}{a^2 + q^2 l^4} \quad (1)$$

where $a = (A_{\text{eff}}/2\pi\gamma)^{1/2}$.

A_{eff} is the effective Hamaker constant of the whole system and γ is the surface tension of the liquid film. For a discrete system the wave vector is $q_m = 2m\pi/d$ (q is used for $m = 1$) where d is the grating spacing and m is an integer. The physics of the system is contained in the healing length, a , which represents the relative strength of the van der Waals and surface tension interactions.

Experimental Description

In our case the substrates are symmetric trapezoidal shaped gratings of spacing $d = 1$ and $0.5 \mu\text{m}$ and height $h_0 = 170 \text{ \AA}$. They were prepared from native oxide-covered silicon using standard lithographic methods, and the precise dimensions were measured with atomic force microscopy and X-ray reflectivity.¹¹⁻¹³ The grating structures were found to be very uniform (less than 5% variation) over the entire sample, which was approximately 1 cm^2 . The bare gratings were cleaned by sonicating in toluene, immersion in chromic acid for 24 h, followed by immersion at $80 \text{ }^\circ\text{C}$ in 25% H_2O_2 ammonium hydroxide solution for 10 min, and finally stripping with 15% HF water solution. Between each step the substrates were rinsed thoroughly with distilled water and dried in vacuum at $150 \text{ }^\circ\text{C}$ for 1 h.

PS films of different molecular weights ($M_w = 600\text{K} - 2000\text{K}$; polydispersity 1.06) and thickness ranging between $l = 179 \text{ \AA}$ and $l = 1100 \text{ \AA}$ were spun cast onto glass substrates from toluene solution. The films were then floated onto cleaned gratings from the water surface and annealed under vacuum of 10^{-4} Torr at $170 \text{ }^\circ\text{C}$ for various times. Test films were also spun cast onto flat Si wafers so their thickness following annealing could be accurately measured by ellipsometry.

The conformality of the polymer films was investigated with atomic force microscopy (AFM) using a di nanoscope III in the contact mode. A minimized contact force of ca. 300 nN was used in order to confirm that no distortion was introduced by the AFM tips. The amplitude of the surface modulation was averaged within $15 \times 15 \mu\text{m}^2$ images taken from at least five different locations on a sample surface. The same samples were also studied with synchrotron X-ray reflection for two reasons: (a) One can compare directly with the AFM measurements and determine if any artifacts are produced due to finite tip size. (b) The X-ray beam can average over a large sampling area (beam width is approximately 1 mm) compared to the grating spacing. The scattered X-ray intensity was measured in reciprocal space for fixed $q_x = q_m$ ($m = 0-4$) in the q_z direction, i.e., along the rods corresponding to various diffraction orders. These scans are sensitive to the periodic structure of the substrate and the modulation of the adsorbed PS films. Furthermore, the intensity along the rods between the diffraction orders was monitored to obtain the diffusely scattered intensity. The diffuse contribution was subtracted from the data for $q_x = q_m$ to obtain the true specular reflectivity and true intensity of the diffraction orders, respectively. In this manner, the intensities from the periodic conformal part of the interfaces were clearly separated from the signal of the random roughness. The X-ray measurements were in good agreement with the AFM, and therefore, we hereafter will mainly discuss the results of AFM. A detailed description of the X-ray scattering theory and experiments can be found in refs 16 and 17.

Roughness Conformality

Parts a and b of Figure 1 show AFM images obtained from a bare grating and a PMMA ($M_w = 330\text{K}$), 750 \AA thick film floated and annealed for 72 h on top of a grating 170 \AA high. From the figure one can see that

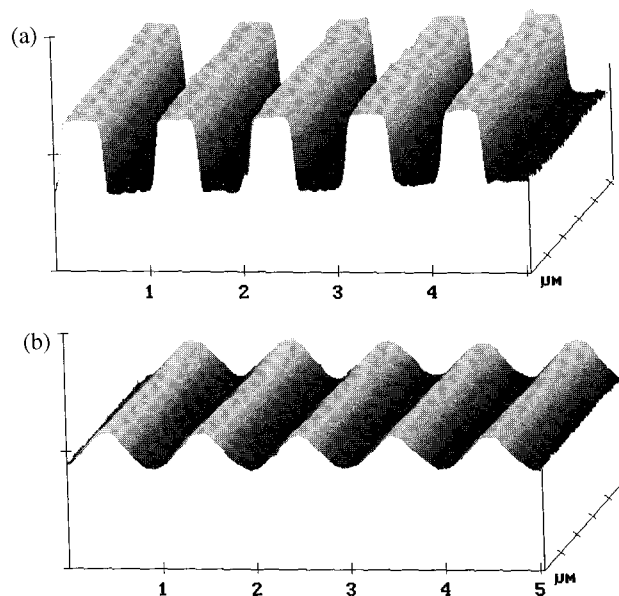


Figure 1. AFM images obtained from (a) the bare trapezoidal grating with $h_0 = 170 \text{ \AA}$ and (b) the same grating covered with a PMMA ($M_w = 330\text{K}$) film, 750 \AA thick, which was annealed for 72 h.

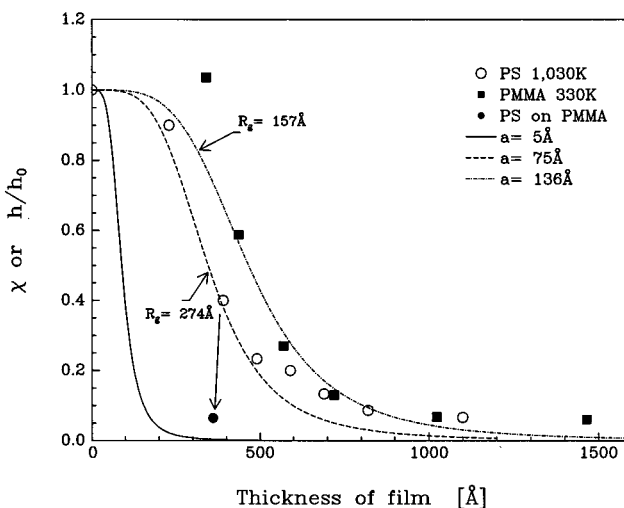


Figure 2. $\chi(q, l)$ ($q = 2\pi/d$) as a function of film thickness on Si gratings $d = 1 \mu\text{m}$ and $h_0 = 170 \text{ \AA}$. AFM measurements: (○) PS (1030K); (■) for PMMA (330K); (●) for a PS film on a PMMA (235 Å) covered grating. The dashed, solid, and dashed-dot lines are AJR predictions for $a = 5$ (corresponding for a simple liquid), 75, and 136 Å, respectively.

the trapezoidal conformation on the grating is reduced to a sinusoidal modulation with an amplitude of 115 \AA on the polymer film surface. This result is in good agreement with eq 1 and the X-ray rod scans,¹⁴ which show that the higher harmonics are rapidly attenuated on the outermost surface of the film. Therefore the amplitude of the quasi-sinusoidal modulation approximately represents the first moment of the Fourier transform and can be compared directly with the AJR theory.

The ratio of the surface modulation amplitude of PS and PMMA thin films to the grating height, h/h_0 , is plotted as a function of film thickness in Figure 2 (open circles). In all cases the PS and PMMA films were annealed at $170 \text{ }^\circ\text{C}$ for 150 and 500 h, respectively. Further annealing for up to 2 weeks produced no significant changes, and hence these modulations were

assumed to be the equilibrium conformations. [It should be noted that the surface states may actually be metastable. As we will discuss later, the amplitude of the modulation is dependent on having chains bound to the surface. The nature of the interaction between PS and silicon oxides is not known, and the PS may eventually desorb from the Si with a time constant longer than the experimental observation time.] From the figure it can be seen that the thinner films follow the substrate or $\chi(q,l) = 1$, whereas with increasing film thickness, $\chi(q,l)$ goes to zero gradually. The amplitudes measured with X-ray reflection¹⁴ on PS films were in good agreement with the present results, which directly prove that the modulation amplitudes can be accurately determined on the polymer surface with the AFM in the contact mode.

The dashed line in Figure 2 corresponds to the AJR model for a simple liquid with $a \approx 5 \text{ \AA}$ in eq 1. This value of a was obtained by substituting the Hamaker constant, $A_{\text{eff}} \approx 5 \times 10^{-13} \text{ erg}$ ($\sim 8.4 k_{\text{B}}T$ for the annealing temperature used) calculated for the system Si/SiO/PS and the surface tension of PS (and PMMA) at $170 \text{ }^\circ\text{C}$,⁴ $\gamma = 30 \text{ erg/cm}^2$. From the figure one can see that, as intuitively expected, in the case of a simple liquid the surface roughness is almost completely attenuated for a film whose thickness is only slightly larger than the grating height. The roughness at the surface of the polymer films, on the other hand, is largely attenuated only after a film thickness more than *four times* the height of the grating. For PS this thickness corresponds to approximately $2R_{\text{g}}$, the polymer radius of gyration, given by $R_{\text{g}} = 6.7 \text{ \AA}(N/6)^{1/2}$ where N is the polymerization index and $R_{\text{g}} = 274 \text{ \AA}$ for PS for molecular weight 1.03M. The dashed line through the data points of the PS film is a fit to eq 1 with $a = 75 \text{ \AA}$ as the only free parameter. Hence the attenuation function for the PS films has the same functional form as that for a simple liquid, but with an effective interaction distance that is approximately 25 times greater.

We can introduce a surface confinement term into the AJR expression due to pinning of the polymer chains via interactions with the Si surface.^{7,11} The free energy per unit area for a polymer film confined on the grating into a thickness, $l < R_0$, where $R_0 = 6.7 \text{ \AA}$ is the end to end distance of the polymer chain, or in this case 671 \AA , is then given by

$$F = \gamma + \frac{A_{\text{eff}}}{12\pi l^2} + \frac{\pi^2}{6} nk_{\text{B}} T \frac{R_0^2}{l^2} \quad (2)$$

where n is the number of chains/unit area. For the general case of adsorbed chains, the functional form of eq 1 remains the same, except that the term a can now be replaced by

$$a = [(A_{\text{eff}} + 12\pi nk_{\text{B}} TR_0^2)/\gamma]^{1/2} \quad (3)$$

In a thin film of entangled chains near a moderately attractive surface, a pseudo-Gaussian chain near a wall will have $N^{1/2}$ contacts with the surface.¹⁹ If these contacts are irreversible on the scale of the experiment, then the layer is essentially a cross-linked membrane whose elastic energy can be approximated by⁷ $(\pi^2/6)k_{\text{B}} T n(R_0^2/l^2 - 1)$. Substituting R_0 for PS of $M_w = 1030\text{K}$ and $l = 300 \text{ \AA}$ leads to $a = 100 \text{ \AA}$, which is in good agreement with our observation of $a = 75 \text{ \AA}$.

In case of a noninteracting surface, the chains are free to move along the surface. Aussere,⁴ Granick, and de Gennes⁶ have shown that no additional force is required to compress the chains and hence $\chi(q,l)$, for polymer melts should reduce to that for simple liquids as predicted by the AJR theory.

To simulate a weakly interacting surface, a PS film (360 \AA thick, $M_w = 1030\text{M}$) was floated on top of a grating covered with a thin (235 \AA) film of polymethyl methacrylate (PMMA, $M_w = 262\text{K}$). PMMA and PS are highly immiscible,^{5,23} and hence no interdiffusion between the two films occurs. Mass transport to smooth out the surface is only possible by motion of the PS molecules within the PS film and along the PS/PMMA interface. The PMMA layer remains pinned at the silicon interface and screens out the interaction from the Si surface in the PS overlayer. AFM microscopy shows that the bilayer covered surface has a modulation of only 6 \AA . after annealing for only 15 h or 1/10 of the time as films of PS or PMMA of equivalent total thickness. From Figure 2 (filled circle), we see that in the absence of pinning by surface interaction, the experimental data now approach the AJR prediction for a small molecular liquid with the correct Hamaker constant for pure van der Waals interactions.

PMMA is more polar than PS and hence is known to interact more strongly with silicon surfaces.¹⁵ The attenuation of the surface roughness, as a function of film thickness, is plotted in Figure 2 (squares). From the figure we can see that the grating height is attenuated far less with film thickness than that the case of PS. In addition, the attenuation length is much larger than $2R_{\text{g}}$, where R_{g} of the PMMA used is 157 \AA . In this case, the roughness is somehow propagated through chains that are not in direct contact with the surface. Confinement effects on polymer chains at distances larger than $2R_{\text{g}}$ (where only a few chains still have surface contacts) were previously reported by Zheng et al.¹¹ where he observed a large decrease in the tracer diffusion coefficient near the silicon interface. The same decrease was observed for the PMMA diffusion coefficient on the grating and will be discussed in the next section.²² Except for the first point, which is not included in the fit,⁶ the dashed line is a fit to the PMMA data with eq 1. In this case as well, the functional form is similar to the AJR model but with an even higher value of a . The value obtained, $a = 136 \text{ \AA}$, indicates that the surface confinement energy of PMMA is roughly four times larger than that of PS.

Lateral Surface Diffusion

When the polymer films are initially floated onto the grating surface, the corrugation at the surface of the films is almost identical to that of the original grating. The attenuation of the original roughness to its equilibrium value occurs over a period of time through center of mass motion of the polymer chains along the grating surface (Figure 3). It has previously been shown by Zheng et al.¹¹ that even a moderately weak surface interaction, such as the one between PS and Si or even the van der Waals interaction between PS and another polymer, can dramatically decrease the diffusion coefficient of polymer chains near the surface. This effect should also be observable in the polymer dynamics leading to the equilibrium surface corrugation of the films on the gratings. Consequently, this may provide a convenient method for measuring the surface diffusion

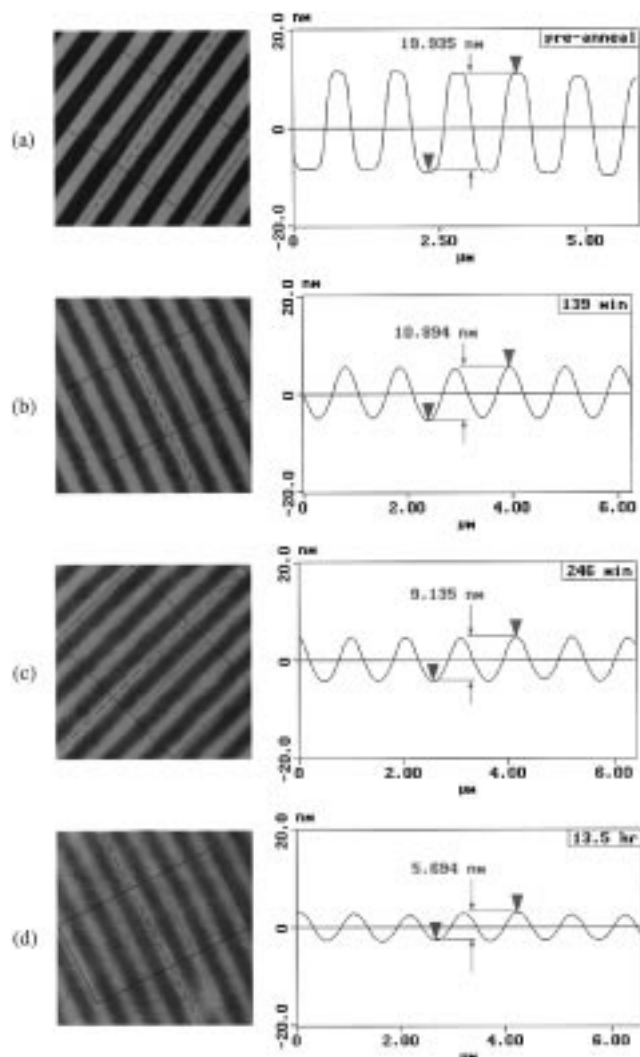


Figure 3. AFM cross sectional scans used to measure h for a PS film of $M_w = 1450K$, $l = 750 \text{ \AA}$ floated on a grating with $d = 10\,560 \text{ \AA}$ and $h_0 = 170 \text{ \AA}$ annealed for various times.

coefficients of polymers without the need for deuteration, floating, or a scattering analysis facility.

In Figure 3 we show AFM cross sectional scans of a PS film of $M_w = 1450K$ and $l = 750 \text{ \AA}$ floated on a grating with $d = 10\,560 \text{ \AA}$ and annealed for various times. Note that the film follows the trapezoidal form of the grating prior to annealing. In Figure 4a we plot $\ln(h/h_0)$ vs annealing time for the PS film. The decrease in amplitude observed in the figure seems to occur in two stages. The first stage, (0–4 h) is too rapid for us to observe in detail experimentally and may be driven by release of elastic strains incurred when the film, initially spun on a flat surface, is stretched across the grating. The second stage is much slower and may be analyzed according to the surface smoothing theory developed by Mullins which is commonly used to study the mechanism of surface diffusion in crystalline solids.^{17–19} In the following we show that this technique is applicable for viscoelastic complex liquids as well.

The amplitude of a sinusoidal wave, $h(t)$, on a surface decays exponentially with annealing time according to

$$h(t) = h_0 \exp[-(-Fq - Aq^2 - Dq^3 - Bq^4)t] \quad (4)$$

where $q = 2\pi/d$ and the coefficients F , A , D , and B describe the contributions of the following transport

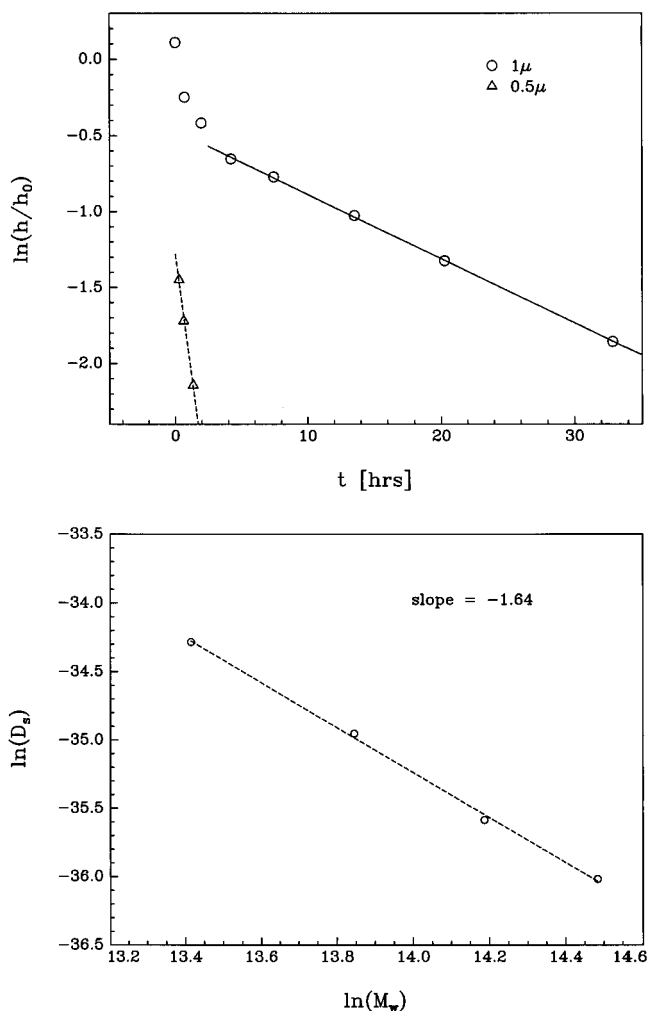


Figure 4. (a) $\ln(h/h_0)$ of the polystyrene film surface shown in Figure 3 plotted as a function of annealing time. The solid and dashed lines are linear fits for 1 and 0.5 μm spaced gratings with slopes of -0.042 and -0.652 respectively. (b) The $\ln(D_s)$ vs $\ln(M_w)$ for PS films (750 \AA thick) on a $d = 1 \mu\text{m}$ grating. The slope of the linear fit is -1.64 .

mechanisms: viscous flow, evaporation and condensation, volume diffusion, and capillary surface diffusion, respectively. Only high molecular weight polymers were used in this study; thus, the evaporation/condensation term can be neglected ($A = 0$).

In order to distinguish between the remaining terms, the dependence of the slope on the grating period, q , was measured. The dashed line in Figure 3a corresponds to the decrease in amplitude under identical annealing conditions of a PS film, 750 \AA thick, floated on a grating having $d = 5,010 \text{ \AA}$. Best fits to the data yields a slope, S , which is approximately 15.5 times greater than the one measured on the grating with $d = 10\,560 \text{ \AA}$ (solid line). This eliminates the first term, which scales as q , and favors the last term, which scales as q^4 . Since only two grating frequencies were available in this study we can not conclusively eliminate the volume term which scales as q^3 . For now we can only assume that since the films are thin, (less than $2R_0$), it is reasonable that the surface term dominates or $B \gg D$. This assumption will be probed in a later study for which a grating with multiple frequencies is being designed.²² Hence capillary flow rather than viscous flow appears to be the predominant mechanism for surface diffusion at long times. This result is consistent

with the initial assumptions of the AJR theory that the equilibrium surface structure is determined by the balance between capillary, van der Waals, and surface-confining forces.

We can now extract the surface diffusion coefficient by measuring the time decay of the surface modulation on the film using

$$h(t) = h_0 e^{-Bq^4} \quad (5)$$

Applying Mullins formalism for surface diffusion in crystalline solids to the case of an entangled polymer melt yields the coefficient

$$B = \gamma \Omega^{4/3} D_s / kT \quad (6)$$

Here D_s is the self-diffusion coefficient near a surface given in the modified reptation model¹¹ by

$$D_s = kTN_e / N^{3/2} (f + f_0 N^{1/2}) \quad (7)$$

where N_e is the average number of monomers between entanglements, f_0 and f are the polymer friction coefficients in the bulk and at the surface, and Ω is the scale factor which determines the dimensions of the diffusion process. In the case of crystalline solids Ω is defined in terms of the free atomic volume which occurs when a surface vacancy is formed. For an entangled polymer we will make the assumption that the surface scaling unit is the tube diameter, L_e which yields

$$\Omega = L_e^3 \quad (8a)$$

$$L_e = aN_e^{1/2} \quad (8b)$$

where a and N_e are, respectively, the statistical segment length and the number of monomers between entanglements for a given polymer. The diffusion coefficient can now be measured by fitting the slope of $\ln(h/h_0)$ vs annealing time and substituting the value into eqs 6 and 8. In order to test this procedure, we will compare both the scaling and the absolute magnitude calculated from eqs 6 and 8 with previous measurements of the diffusion coefficients using standard ion scattering methods.

Figure 4b is a log-log plot of the surface diffusion coefficient vs the molecular weight for PS thin films on a $d = 10\,560$ Å grating, using a constant film thickness of 750 Å. The slope, -1.6 ± 0.1 , is in good agreement with the molecular weight dependence of the diffusion coefficient normal to a silica surface found by Zheng et al.¹¹ and predicted in eq 7 for polymer chains in contact with a strongly interacting surface ($f \gg f_0$). Substituting, for PS,²⁴ $N_e = 173$, $a = 6.7$ Å, $L_e = 88$ Å, and $\gamma(T = 170^\circ\text{C}) = 30$ erg/cm² into eqs 6, 7, and 8 we obtain $D_s = 6.5 \times 10^{-16}$ cm²/s for the $M_w = 1030K$ PS film shown in Figure 4b. This value is approximately 1 order of magnitude smaller than the self-diffusion coefficient of PS in the bulk²³ and is consistent with the assumption that strong interactions confine the polymer chains and require additional terms in the equation for the free energy (eq 2). The magnitude of D_s is in good agreement with Zheng's measurement using DSIMS^{11,20,21} indicating that no significant difference exists between diffusion along (parallel) or away (normal) from an interacting surface, or the effect of trapping on the dynamics is isotropic.

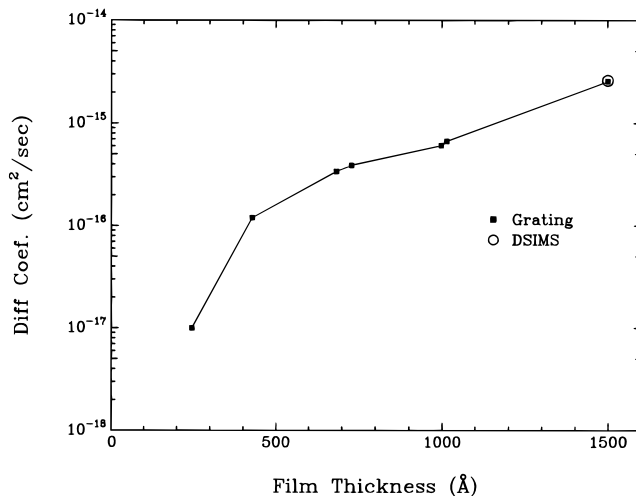


Figure 5. Diffusion coefficients measured on the grating shown in Figure 1a for PMMA ($M_w = 112\,000$) films plotted as a function of film thickness. The open circle corresponds to the tracer diffusion coefficient as measured by DSIMS in ref 23.

In the case of the PMMA films we used the corrugation decay method to measure the dependence of D_s on film thickness, or distance from the interacting Si grating surface. Figure 5 is a logarithmic plot of the diffusion coefficients vs film thickness obtained from PMMA films of $M_w = 112\,000$ ($M_w/M_n = 1.04$). From the figure we can see that the diffusion coefficients decrease by almost 2 orders of magnitude as the Si surface is approached. From the figure we can see that one requires films whose thickness is greater than approximately $6R_g$, (where $R_g = 110$ Å) before one observes the bulk diffusion coefficient. A similar dependence for D on the distance from the Si surface was previously measured by Zheng et al. using DSIMS for PS films.²³ On the basis of experiments with PS films, Zheng et al.²³ have suggested that this phenomena may be explained by a two-fluid model where the polymer liquid layer adjacent to the reactive surface acts as an effective cross-linked gel which can trap the adjacent "bulk" liquid layer retarding its motion. Unfortunately, no quantitative model explaining these phenomena has yet been proposed.

The magnitude of the diffusion coefficients plotted in Figure 5 was calculated by substituting the parameters for atactic PMMA,²⁴ $N_e = 57$ and $a = 7.4$ Å into eqs 6 and 8. The open square point corresponds to the diffusion coefficient as measured by dynamic secondary ion mass spectrometry (DSIMS) at a distance of 1600 Å from the Si interface.²² The value of $D_s = 26 \times 10^{-16}$ cm²/s is in good agreement with that measured by the amplitude attenuation method. This indicates that at least for the two polymers studied that tube diameter is indeed a reasonable scaling factor for entangled polymer films.

In conclusion we have shown that the confinement of polymer chains by strong surface interactions can propagate the substrate roughness over distances much larger than those observed in simple liquids. This phenomenon can be explained by assuming that the chains are confined to the surface by a strong interaction and introducing an additional term in the free energy. This term is inversely proportional to the square of the film thickness and hence does not change the functional form of the attenuation equation derived for a simple

liquid. Reducing the surface interaction by covering the bare silicon surface restores the simple liquid behavior even for polymer films.

By adapting the classic smoothing theory of Blakely and Mullins¹⁷⁻¹⁹ to polymer dynamics, we show that we can extract surface diffusion coefficients from polymer melts from the time dependence of the roughness amplitude. The results are in good agreement with previous DSIMS measurements of diffusion normal to the silicon surface.¹¹ The measured diffusion coefficients depend on the distance from the silica interface and scale as $M_w^{3/2}$; confirming the existence of strong surface interactions.

Acknowledgment. Support from the NSF (DMR-9316157), NSF-MRSEC (DMR9632525), and DOE (DE-FG02-93ER45481) is gratefully acknowledged.

References and Notes

- (1) Feng, Y. P.; Sinha, S. K.; Deckman, H. W.; Hastings, J. B.; Siddons, D. P. *Phys. Rev. Lett.* **1993**, *71*, 537.
- (2) Tidswell, I. M.; Rabedeau, T. A.; Pershan, P. S.; Kosowsky, S. D. *Phys. Rev. Lett.* **1991**, *66*, 2108.
- (3) Andelmann, D.; Joanny, J.-F.; Robbins, M. O. *Europhys. Lett.* **1988**, *7*, 731.
- (4) Ausserré, D. *J. Phys. Fr.* **1989**, *50*, 3021.
- (5) Hu, H.; Granick, S.; Schweizer, K. S. *J. Non-Cryst. Solids* **1994**, *172*, 721.
- (6) de Gennes, P. G. *Hebd. C. R. Acad. Sci. Paris* **1980**, *290*, 509; **1987**, *305*, 1181.
- (7) Zhao, W.; Rafailovich, M. H.; Sokolov, J.; Fetters, L. J.; Plano, R.; Sanyal, M. K.; Sinha, S. K.; Sauer, B. B. *Phys. Rev. Lett.* **1993**, *70*, 1453. Sauer, B. B. Private communication.
- (8) Liu, Y.; Rafailovich, M. H.; Sokolov, J.; Schwarz, S. A.; Zheng, X.; Eisenberg, A.; Kramer, E. J.; Sauer, B. B.; Satija, S. *Phys. Rev. Lett.* **1994**, *73*, 440.
- (9) Israelachvili, J. N.; *Intermolecular and Surface Forces*, Academic Press New York, **1985**.
- (10) Robbins, M. O.; Andelmann, D.; Joanny, J.-F. *Phys. Rev.* **1991**, *A43*, 4344.
- (11) Hansen, W.; Kotthaus, J. P.; Merkt, U. *Nanostructured Systems, Semiconductors and Semimetals 35*; Academic Press: New York, 1992; p 279.
- (12) Heitmann, D.; Kotthaus, J. P. *Phys. Today* **1993**, *46*, 56.
- (13) Tolan, M.; Vacca, G.; Sinha, S. K.; Li, Z.; Rafailovich, M. H.; Sokolov, J.; Lorenz, H.; Kotthaus, J. P. *J. Phys. D: Appl. Phys.* **1995**, *28*, A231.
- (14) Tolan, M.; Vacca, G.; Wang, J.; Sinha, S. K.; Li, Z.; Rafailovich, M. H.; Sokolov, J.; Gibaud, A.; Lorenz, H.; Kotthaus, J. P. *Physica B (Amsterdam)* **1996**, *221*, 53.
- (15) Granick, S. In *Physics of Polymer Surfaces and Interfaces*; Sanchez, I. C., Ed.; Butterworth-Heinemann Publ.: Singapore, 1994.
- (16) It was shown clearly with atomic force microscopy that the polymer thin films form an initial conformal modulation automatically, the height of which is observed to be higher than that of the bare substrate. This effect is not well understood and may be due to strains related to the floating procedure. This elastic strain relaxes quickly as addressed in the diffusion section. The relaxation however may require much longer times for very thin PMMA films, and the data point is not at equilibrium. Consequently it was not included in the data analysis.
- (17) Maiya, P. S.; Blakely, J. M. *Appl. Phys. Lett.* **1965**, *7*, 60.
- (18) Mullins, W. W. *Metal Surfaces*; Amer. Soc. for Metals: Metals Park, OH, 1963.
- (19) Bonzel, H. P. In *Surface Mobilities on Solids Materials*; Binh, V. T., Ed.; NATO ASI Series 86; Plenum: New York, 1983.
- (20) Zheng, X. Ph.D. Thesis, SUNY at Stony Brook, 1996.
- (21) Green, P. F.; Kramer, E. J. *J. Mater. Res.* **1986**, *1*, 202.
- (22) Kharas, D.; Krausch G.; Rafailovich, M. H.; Sokolov, J.; Tolan, M.; Schwarz, S. A.; Strzhemechny, Y. Manuscript in preparation.
- (23) Zheng, X.; Rafailovich, M. H.; Sokolov, J.; Strzhemechny, Y.; Schwarz, S. A.; Sauer, B. B.; Rubinstein, M. *Phys. Rev. Lett.* **1997**, *79*, 241.
- (24) Higgins, J.; Stein, R. S. *J. Appl. Crystallography* **1978**, *11*, 346.

MA970977X